Identification of in Vivo Phosphorylation Sites of MLK3 by Mass Spectrometry and Phosphopeptide Mapping†

Panayiotis O. Vacratsis,‡,§ Brett S. Phinney,‡ Douglas A. Gage,‡ and Kathleen A. Gallo*,‡,||

Department of Biochemistry and Molecular Biology and Department of Physiology, Michigan State University, East Lansing, Michigan 48824

Received December 20, 2001; Revised Manuscript Received February 25, 2002

ABSTRACT: MLK3 is a serine/threonine protein kinase that functions as an upstream activator of the JNK pathway. Previous work has suggested that MLK3 is a multiphosphorylated protein. In this study, mass spectrometry coupled with comparative phosphopeptide mapping was used to directly characterize MLK3 in vivo phosphorylation sites. Various types of mass spectrometry were used to analyze MLK3 tryptic peptides separated by C18 reverse-phase HPLC, leading to the identification of Ser^{524}, Ser^{654}, Ser^{705}, Ser^{740}, Ser^{758}, Ser^{770}, Ser^{793}, and a site found on peptide $Ser^{11}-Arg^{37}$ within a Gly-rich region as MLK3 phosphorylation sites. Additionally, porous graphitic carbon chromatography successfully retained and resolved phosphopeptides that had eluted along with nonvolatile salts and buffers in the flowthrough fractions from the C18 column. Following resolution by PGC chromatography, MALDI-MS in conjunction with alkaline phosphatase treatment identified Ser^{555}, Ser^{556}, Ser^{724}, and Ser^{727} as sites of phosphorylation on MLK3. A proline residue immediately follows 7 of the 11 unambiguously identified phosphorylation sites, suggesting that MLK3 may be a target of proline-directed kinases. Finally, two-dimensional phosphopeptide mapping confirmed that phosphorylation of Ser^{555} and Ser^{556} of MLK3 is induced by the activated small GTPase Cdc42.

Mixed-lineage kinase 3 (MLK3)[1] (*1*−*3*) is an intracellular serine/threonine kinase that has been identified as an upstream activator of the c-Jun NH_2-terminal kinase (JNK) pathway (*4*−*7*). Specifically, MLK3 functions as a mitogen-activated protein kinase kinase kinase (MAPKKK), capable of phosphorylating and activating the JNK activators MKK4 and MKK7 (*8*). The JNK scaffold proteins JIP 1−3 have been shown to associate with MLK3, as well as with MKK7 and JNK (*9*, *10*). JIP has been implicated in facilitating MLK3-mediated JNK activation (*9*). In addition to its established role as an upstream activator of the JNK pathway, a recent report has shown that overexpressed MLK3 is capable of activating the NF-κB pathway in T cells. Hehner et al. demonstrated that overexpressed MLK3 increases the transcriptional activity of NF-κB and phosphorylates inhibitor of NF-κB kinase (IKK). Thus, MLK3 may act as an IKK kinase to positively regulate the NF-κB pathway (*11*). Although not completely defined, recent data have emerged describing physiological processes that MLK3 may regulate. In addition to being a potential regulator of T cell receptor signaling (*12*−*14*), MLK3 and other MLKs have been implicated in JNK-mediated neuronal apoptosis (*15*−*18*).

Our laboratory has focused on delineating the molecular mechanisms that regulate MLK3 activity (*19*−*21*). MLK3 contains several protein−protein interaction domains that may be important for regulation of the kinase, including an SH3 domain, a leucine zipper domain, a Cdc42/Rac interactive binding (CRIB) motif, and a COOH-terminal region of 220 amino acids that is rich in proline, serine, and threonine residues. We recently published that MLK3 is autoinhibited through an intramolecular interaction between its SH3 domain and a nonclassical SH3 binding sequence located between its zipper and CRIB motifs (*21*). MLK3 associates with an activated form of the GTPase Cdc42 (*22*), and coexpression of MLK3 and activated Cdc42 in cells increases the catalytic activity of MLK3 (*23*, *24*). Furthermore, we have shown that coexpression of MLK3 with activated Cdc42 alters the in vivo phosphorylation pattern of MLK3 (*23*).

Phosphorylation is a dominant mechanism in the regulation of protein kinases. A precise mechanistic understanding of how site-specific phosphorylation regulates MLK3 first requires the identification of those sites. Based on site-directed mutagenesis studies, Thr^{277} and Ser^{281} in the

† This work was supported by a grant from the National Institutes of Health (CA76306) to K.A.G.

* To whom correspondence should be addressed at the Departments of Physiology and of Biochemistry and Molecular Biology, Michigan State University, 4180 Biomedical and Physical Sciences Building, East Lansing, MI 48824. Tel.: 517-355-6475; Fax: 517-355-5125; Email: gallok@msu.edu.

‡ Department of Biochemistry and Molecular Biology.

§ Present address: Department of Biological Chemistry, University of Michigan Medical School, M4433 Med Sci I, Ann Arbor, MI 48109-0606.

|| Department of Physiology.

[1] Abbreviations: MLK, mixed-lineage kinase; JNK, c-Jun NH_2-terminal kinase; MAPKKK, mitogen-activated protein kinase kinase kinase; Il-2, interleukin-2; IKK, inhibitor of NF-κB kinase; CRIB, Cdc42/Rac interactive binding; HPK-1, hematopoietic progenitor kinase-1; MS, mass spectrometry; MALDI-TOF, matrix-assisted laser desorption/ionization-time-of-flight; ESI−CID, electrospray ionization−collision-induced dissociation; PBS, phosphate-buffered saline; RP-HPLC, reverse-phase high-pressure liquid chromatography; TLC, thin-layer chromatography; PGC, porous graphitic carbon; TLE, thin-layer electrophoresis; PAA, phosphoamino acid analysis; PSD, post source decay; WT, wild type.

10.1021/bi016075c CCC: $22.00
Published on Web 04/06/2002

activation loop of MLK3 have been suggested to be major phosphorylation sites critical for MLK3 activation (*25*). However, at present, no MLK3 phosphorylation sites have been directly identified.

In this study, a combination of different mass spectrometric techniques were employed to identify in vivo phosphorylation sites of MLK3. Mass spectrometry (MS) has proven to be a valuable analytical tool, due to its high mass accuracy, to study posttranslational protein modifications including identification of phosphorylation sites on proteins. Recent advances have made mass spectrometry sensitive enough to study modified proteins from in vivo sources, although phosphorylation site turnover rates and low amounts of phosphorylated material can still pose a technical challenge. Using matrix-assisted laser desorption/ionization (MALDI)-MS and electrospray ionization−collision-induced dissociation (ESI−CID) MS coupled with phosphopeptide mapping, 12 in vivo MLK3 phosphorylation sites were identified. This work provides the critical information for embarking on investigation of the mechanistic basis of site-specific phosphorylation in the regulation of MLK3 and its signaling pathways.

EXPERIMENTAL PROCEDURES

DNA Constructs and Mutagenesis. Construction of the cytomegalovirus-based expression vectors carrying the cDNAs for wild-type MLK3 (pRK5-*mlk3*) has been described elsewhere (*22*). The expression plasmid encoding NH_2-terminal Flag epitope-tagged constitutively active Cdc42 (pRK5-Nflag.*cdc42*^{V12}) was kindly provided by Avi Ashkenazi (Genentech). The expression plasmid containing the wild-type *mlk3* cDNA was used as a template to create two single mutants (*mlk3* S740A and *mlk3* S740E) and two double mutants (*mlk3* S555E/S556E and *mlk3* S724A/S727A) using the Quick Change Site-Directed Mutagenesis Kit (Stratagene, La Jolla, CA). The presence of the desired mutation was confirmed by automated DNA sequencing.

Cell Culture, Transfections, and Lysis. Human fetal kidney 293 cells (6×10^7) were maintained in Ham's F12:low-glucose Dulbecco's-modified Eagle's media (1:1) (Gibco BRL) supplemented with 8% fetal bovine serum (Gibco BRL), 2 mM glutamine, and penicillin/streptomycin (Gibco BRL). Cells were transiently transfected with plasmids using the calcium phosphate technique, and lysed as previously described (*23*).

In Vivo Labeling with [^{32}P]Phosphate. Following a 14 h cotransfection of pRK5-*mlk3* and pRK5-Nflag.*cdc42*^{V12}, 293 cells (2×10^6) were washed 5 times with phosphate-free medium [Dulbecco's-modified Eagle's medium supplemented with 10% dialyzed FBS (Summit Biotechnology)], and incubated at 37 °C for 2 h. The cells were then incubated in serum-containing phosphate-free medium containing 1 mCi/mL ^{32}P carrier-free orthophosphate (NEN Life Science Products) for 4 h at 37 °C.

Immunoprecipitation and in-Gel Trypsin Digestion. MLK3 antiserum (0.25 μg/μL slurry) was prebound to protein A−agarose beads. Immunoprecipitation experiments were performed essentially as described previously (*23*) except that the cleared cellular lysates from 6×10^7 cells were immunoprecipitated overnight. The immunoprecipitates of MLK3 from the nonradiolabeled sample (from 6×10^7 cells) and the radiolabeled sample (from 2×10^6 cells) were combined, and the proteins were separated by SDS−PAGE. Gels were rinsed in PBS and dried. Incorporation of radioactivity was detected by phosphorimaging (Molecular Dynamics).

Radiolabeled MLK3 bands were excised from the dried SDS−PAGE gel and rehydrated with water (4 μL). The gel pieces were washed twice with 500 μL of 0.1 M ammonium bicarbonate containing 50% acetonitrile at 30 °C for 50 min. The gel pieces were then completely dried under a gentle stream of N_2. The gel pieces were partially rehydrated with 4 μL of 0.1 M ammonium bicarbonate containing 0.02% Tween-20. Sequencing-grade trypsin (2 μg) (Roche) was immediately administered to the gel pieces. Complete hydration was achieved by adding 40 μL of digestion buffer (50 mM ammonium bicarbonate). Trypsin digestion was performed overnight at 30 °C. The digestion was terminated with 0.1 volume of 10% TFA. The peptides were extracted with two washes of 60% acetonitrile containing 0.1% TFA for 50 min at 30 °C.

Reverse-Phase HPLC. Following SDS−PAGE and in-gel trypsin digestion, the resulting MLK3 peptides were fractionated by microbore reverse-phase HPLC (Michrom) on a C18 column (5 μm, 300 Å, 1.0 × 150 mm) (Vydac). Peptides were eluted with a 0−95% linear gradient of acetonitrile in 0.1% trifluoroacetic acid (TFA) at a flow rate of 50 μL/min. The eluant was monitored by UV absorbance at 214 nm, and peak fractions were collected at approximately 1 min intervals. A 1 μL aliquot of each HPLC fraction was spotted on a thin-layer chromatography (TLC) plate followed by detection of ^{32}P radioactivity using phosphoimaging analysis.

Porous Graphitic Carbon Chromatography. A reverse-phase PGC column (5 μm, 250 Å, 1 × 150 mm) (Keystone Scientific) was used to resolve the poorly retained peptides that eluted in the first 5 min off the C18 column. Conditions for PGC chromatography were identical to those for the C18 separation with the exception that the flow rate was reduced to 20 μL/min. A 1 μL aliquot of each PGC fraction was spotted on a TLC plate, and radioactive spots were detected by phosphorimaging.

Phosphopeptide Mapping. Radiolabeled HPLC fractions (1 μL) were analyzed by one-dimensional thin-layer electrophoresis (TLE) and one-dimensional TLC. The mobility of the radiolabeled peptides under these conditions was used to correlate a HPLC fraction with a spot seen on the two-dimensional map from MLK3 labeled in vivo. The conditions for TLE and TLC have been described in detail elsewhere (*23*).

Phosphoamino Acid Analysis. Selected radiolabeled HPLC fractions (5 μL) were hydrolyzed in 100 μL of 6 N HCl for 1 h at 100 °C. After concentration, the free phosphoamino acids were resolved by one-dimensional TLE in pH 2.5 buffer [66.7% pH 3.5 buffer (glacial acetic acid/pyridine/water, 50:5:945, v/v/v) and 33.3% pH 1.9 buffer] on 20 × 20 cm cellulose TLC plates at 0 °C and 1000 V for 50 min. Unlabeled phosphoamino acid standards (Sigma) and xylene cyanol FF marker dye (Sigma) were used as standards. The unlabeled phosphoamino acids were visualized by ninhydrin staining, and the ^{32}P-labeled phosphoamino acids were visualized and quantitated by phosphorimaging.

MALDI-MS. MALDI-TOF mass spectrometry was performed on a Voyager-DE STR time-of-flight instrument (Applied Biosystems), equipped with a nitrogen laser operating at 337 nm. The HPLC fractions were analyzed in either linear positive mode or reflector positive mode (for PSD analysis) using α-cyano-4-hydroxycinnaminic acid (saturated solution in 50% acetonitrile with 0.1% TFA) as the UV-absorbing matrix. Samples were prepared by mixing 1 μL of sample and 1 μL of matrix solution on the MALDI plate and allowing them to air-dry. All mass spectra were externally calibrated with bradykinin and insulin. Calf intestinal alkaline phosphatase (2 units, New England Biolabs) was incubated with 5 μL of HPLC fractions containing phosphopeptides in 50 mM NH_4HCO_3 at 37 °C for 3 h. The dephosphorylation reaction was terminated by the addition of 50% acetonitrile, and the samples were washed with water and concentrated.

Electrospray Mass Spectrometry. Liquid chromatography/mass spectrometric analysis of selected MLK3 HPLC fractions was accomplished using the Waters CapLC system (Waters Corp., Milford, MA) coupled to an LCQ DECA quadrupole ion trap mass spectrometer (ThermoFinnigan, San Jose, CA) through the Picoview nanospray source (New Objectives, Cambridge, MA). A 0.1−6 μL aliquot of each fraction was trapped on a Michrom CapTrap cartridge (Michrom BioResources, Inc., Auburn, CA) and then backflushed on a 75 μm i.d. × 15 cm Picofrit column packed with 5 μm 100 Å Magic C18AQ material (Michrom BioResources, Inc., Auburn, CA). Peptides were then eluted from the column using a gradient of 5% B to 50% B in 30 min at a flow rate of 250 nL/min. Mobile phase A consisted of 0.1% formic acid while mobile phase B consisted of 0.1% formic acid in a 95:5 acetonitrile/water solution. The Picofrit column made electrical contact through a precolumn ZDV titanium union, and terminated in a 15 μm tip i.d. outlet spray needle. Mass spectra were acquired using the Top3 double-play mode of operation where the three most abundant peptide ions detected in a MS survey scan triggered data-dependent MS/MS fragmentation for obtaining product ion spectra. To identify the peptides in the digest, uninterpreted peptide product ion spectra were searched against a database containing the sequence of MLK3 using the TurboSEQUEST database search program. Searches were done both with and without the digest and posttranslational specificities turned on.

RESULTS

In-Gel Trypsin Digestion of Immunoprecipitated MLK3. Comparative two-dimensional phosphopeptide analyses of in vivo phosphorylated MLK3 and in vitro kinase assays indicate that MLK3 is a multiphosphorylated protein whose activity is increased and whose phosphorylation pattern is altered upon coexpression with activated Cdc42 (Cdc42 V12) (*26*). However, the sites of MLK3 phosphorylation have not been identified. To obtain sufficient quantities of in vivo phosphorylated MLK3 for mass spectrometry analysis, 1×10^8 293 cells expressing MLK3 in the presence of activated Cdc42 were cultured. MLK3 was isolated from cleared cellular lysates by immunoprecipitation with a MLK3 polyclonal antibody. In addition, radiolabeled MLK3 was immunoprecipitated from 4×10^6 293 cells that had been labeled with ^{32}P carrier-free orthophosphate. The radiolabeled and unlabeled samples of MLK3 were combined and further resolved by SDS/PAGE. The gel was dried, and the radiolabeled bands were visualized by phosphorimaging. The radiolabeled band corresponding to the size of MLK3 was excised from the gel and subjected to in-gel digestion with trypsin. The tryptic peptides were extracted from the gel, resulting in 65−80% recovery based on radioactivity using Cerenkov counting.

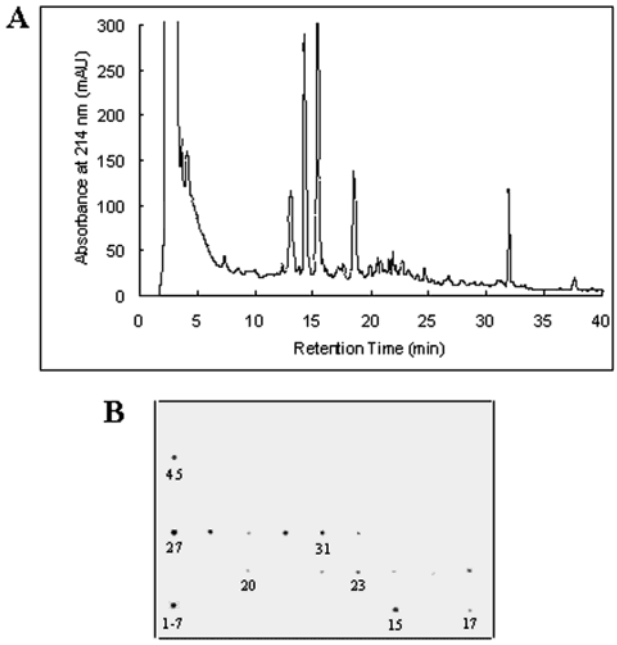

FIGURE 1: Reverse-phase HPLC fractionation of MLK3 tryptic peptides. MLK3 coexpressed in 293 cells with activated Cdc42 was isolated by immunoprecipitation. MLK3 was also isolated from a smaller scale identical culture that had been labeled with [^{32}P]-orthophosphate. The two MLK3 samples were combined and further resolved by SDS/PAGE. The gel was dried, and the MLK3 bands were visualized by phosphorimaging. (A) The MLK3 band was excised from the gel and subjected to in-gel digestion with trypsin. The tryptic peptides were fractionated by reverse phase-HPLC on a microbore C18 column. (B) An aliquot (1 μL) of each HPLC fraction was spotted on a TLC plate and air-dried. Radiolabeled fractions were detected by phosphorimaging.

Separation of Tryptic Peptides by Reverse-Phase HPLC and Phosphopeptide Mapping. A small portion of the recovered peptides was analyzed by two-dimensional phosphopeptide mapping (Figure 2A). The analysis shows the typical in vivo phosphorylation pattern observed for MLK3 coexpressed with activated Cdc42 (spots are labeled *a*−*g*) including the Cdc42-inducible sites (spots are labeled *x* and *y*). The remainder was fractionated by reverse-phase HPLC (Figure 1A). Aliquots of fractions were spotted onto TLC plates and analyzed for the presence of radiolabeled material by phosporimaging (Figure 1B).

HPLC fractions containing radiolabeled material were characterized by one-dimensional TLE and one-dimensional TLC (Figure 2B,C). This analysis allowed for major phosphopeptides labeled on the two-dimensional map in Figure 2A to be correlated with and assigned to an HPLC fraction number.

Identification of Phosphorylation Sites Using MALDI-MS and ESI−CID. HPLC fractions containing radiolabeled phosphate were analyzed by MALDI-MS in the linear positive-ion mode using α-cyano-4-hydroxycinnamic acid as the UV-absorbing matrix. A computer program, MS-

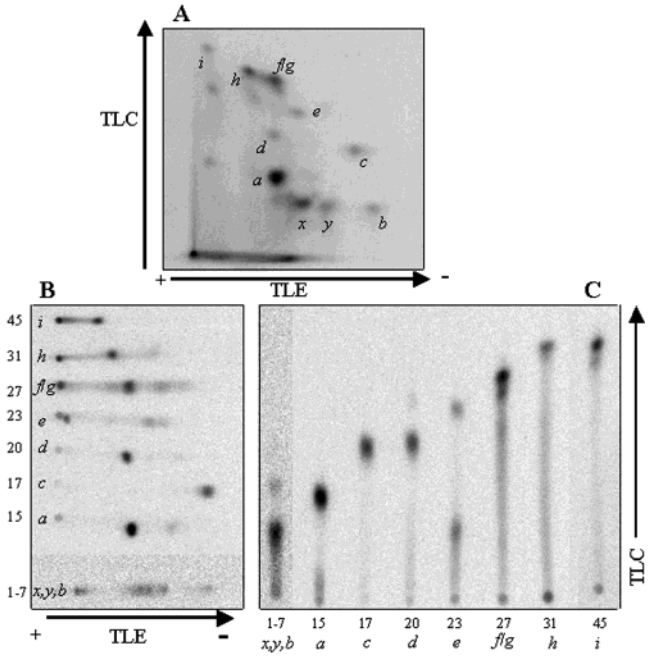

FIGURE 2: One-dimensional phosphopeptide analysis of radiolabeled HPLC fractions. Aliquots of each radiolabeled HPLC fraction were analyzed by TLE and TLC. (A) A reference two-dimensional phosphopeptide map of in vivo labeled MLK3. (B) One-dimensional TLE. (C) One-dimensional TLC. For each radiolabeled sample, the HPLC fraction and the corresponding spot on the two-dimensional phosphopeptide map are labeled.

Digest, was used to calculate the monoisotopic masses of all MLK3 tryptic peptides including phosphorylated peptides and partially digested peptides and to compare those masses with the data generated by MALDI-MS. Samples that potentially contained phosphorylated MLK3 peptides were then incubated with alkaline phosphatase and reexamined by MALDI-MS for the loss of multiples of 80 Da, which corresponds to the loss of a phosphate group. MALDI-MS data that implicated more than one possible MLK3 phosphopeptide, or a peptide that contained multiple phosphorylatable amino acids, were considered ambiguous. Such samples were further analyzed by MALDI−PSD or ESI−CID to obtain sequence information and to identify phosphorylation sites. Further characterization of certain radioactive HPLC fractions was obtained by phosphoamino acid analysis (Figure 3). For this analysis, a 5 μL aliquot was incubated in 6 N HCl for 1 h at 37 °C, and the phosphoamino acid content was examined by one-dimensional TLE.

HPLC Fraction 45. The MALDI-MS spectrum of HPLC fraction 45 (spot *i*) showed two major peaks, at *m*/*z* 2334.59 and at *m*/*z* 2254.73, corresponding to the monophosphorylated and unphosphorylated peptide Thr^{702}−Arg^{723} of MLK3, respectively (Figure 4A). Following alkaline phosphatase treatment of the fraction, only the unphosphorylated peptide was identified. This peptide contains two threonine residues and a single serine residue. Phosphoamino acid analysis (PAA) of this HPLC fraction revealed that the peptide contained exclusively phosphoserine (Figure 3, lane 4). Therefore, Ser^{705} was assigned as a phosphorylation site in MLK3.

HPLC Fraction 23. The MALDI-MS spectrum of HPLC fraction 23 (spot *e*) revealed signals at *m*/*z* 2395.17 and at

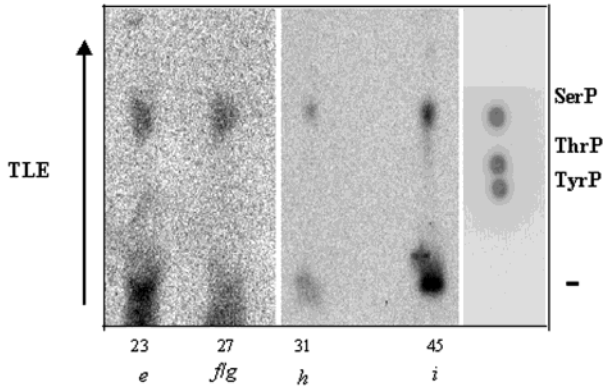

FIGURE 3: Phosphoamino acid analysis of selected HPLC fractions. Aliquots of selected HPLC fractions were hydrolyzed in 6 N HCl at 100 °C for 1 h. The phosphoamino acid content was analyzed by one-dimensional TLE and visualized by phosphorimaging. The positions of phosphoamino acid standards stained with ninhydrin, as well as the position of free inorganic phosphate (Pi, −), are indicated.

2315.94, corresponding to the monophosphorylated and unphosphorylated peptide Ser^{11}−Arg^{37}, respectively (Figure 4B). Phosphatase treatment produced a shift of 80 Da to yield only the unphosphorylated peak. This peptide contains five serines and no threonines. We were unable to obtain sequence information on this peptide by using ESI−CID or MALDI−PSD. Ser^{11}−Arg^{37} resides within a glycine-rich motif, and within this 27 amino acid peptide, 13 glycine residues are present. This high glycine content may be the reason fragmentation of this peptide was unsuccessful.

HPLC Fraction 31. MALDI-MS analysis of HPLC fraction 31 (spot *h*) showed a peak at *m*/*z* 1699.21 (Figure 5A, *a*). Following phosphatase treatment, the peak shifted by −80 Da to 1619.61 (Figure 5A, *b*). The calculated mass values matched two possible monophosphorylated MLK3 peptides: Val^{131}−Lys^{144} and Asn^{515}−Arg^{529}. To distinguish between these two peptides, MALDI−post source decay (PSD) analysis was performed on fraction 31 (Figure 5A, *c*). MALDI−PSD is an extension of linear MALDI-MS that has the potential of obtaining primary sequence information. PSD is a process whereby the precursor ion fragments through metastable decomposition in the flight tube (*27*). MALDI−PSD analysis involves deflecting the ions using an electrically charged reflectron mirror at the end of the flight tube at various mirror voltages to discriminate the ions by flight time dispersion. The resulting spectrum of the precursor ion with its fragment ions provides sequencing information. PSD analysis of fraction 31 revealed a series of COOH-terminal fragment ions (y ions) corresponding to the phosphopeptide Asn^{515}−Arg^{529}. This peptide has one Ser residue (Ser^{524}) and one Thr residue (Thr^{526}). One of the most abundant peaks is y_{15} − 98 Da, which corresponds to the fragmentation of H_3PO_4 from the precursor ion. The y_6 − 98 Da peak corresponds to the peptide fragment Ser^{524}−Arg^{529} with the loss of H_3PO_4. Furthermore, the mass detected for the y_5 ion that contains the Thr residue but not the Ser residue (Pro^{525}−Arg^{529}) corresponds to a unphosphorylated peptide fragment. PAA analysis of HPLC fraction 31 also confirms only Ser phosphorylation (Figure 3, lane 3). Taken together, these data allowed assignment of phosphorylation to Ser^{524}.

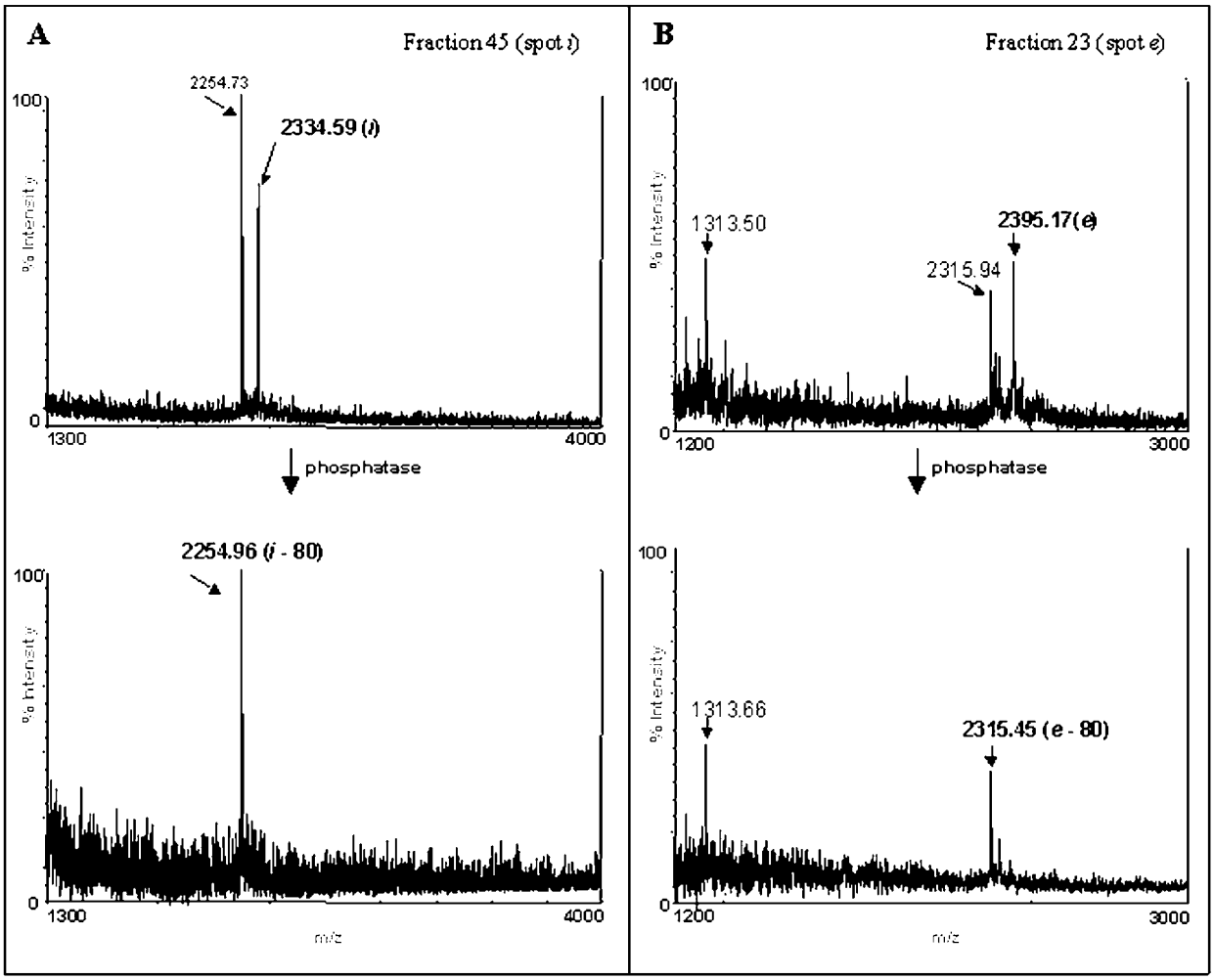

FIGURE 4: Analysis of HPLC fractions 23 and 45 using MALDI-MS combined with alkaline phosphatase treatment. HPLC fraction 45 (spot *i*) (A) and HPLC fraction 23 (spot *e*) (B) were analyzed by MALDI-MS in the linear positive ion mode with α-cyano-4-hydroxycinnamic acid as the UV-absorbing matrix. The *m*/*z* values corresponding to a phosphorylated peptide are indicated in boldface type. The HPLC fractions were then subjected to alkaline phosphatase treatment and reanalyzed by MALDI-MS. The peaks corresponding to dephosphorylated peptides are indicated in boldface with the change in *m*/*z* of −80 corresponding to the loss of a phosphate moiety.

HPLC Fraction 17. Fraction 17 (spot *c*) exhibited one peak in the MALDI-MS spectrum that was reduced by 80 *m*/*z* units following phosphatase treatment, corresponding to a phosphorylated peptide (Figure 5B, *a* and *b*). The *m*/*z* 902.46 peak matched two possible phosphopeptide sequences in MLK3. Therefore, ESI−CID using an ion-trap electrospray instrument was performed. The most prominent peak is the neutral loss of $[H_3PO_4]^{+2}$ (−49 Da) at *m*/*z* 402.5. Analysis of the doubly charged parent ion at an *m*/*z* value 451.9 produced a mixture of b and y series fragment ions that corresponded to the phosphopeptide $Pro^{767}-Arg^{773}$ and allowed assignment of phosphorylation at Ser^{770}, the only phosphorylatable residue in this sequence, as a MLK3 phosphorylation site (Figure 5B, *c*).

HPLC Fraction 27. Phosphopeptides corresponding to spots *f* and *g* eluted in fraction 27. The MALDI-MS spectrum of fraction 27 contained four peaks, which shifted by −80 Da following phosphatase treatment (Figure 6A). Phosphoamino acid analysis of fraction 27 revealed only phosphoserine (Figure 3, lane 2). Analysis of the calculated mass values matched two possible MLK3 monophosphorylated peptides ($Ala^{532}-Arg^{550}$ and $Leu^{640}-Arg^{659}$) to the value at *m*/*z* 2171.93. We were unable to obtain sequence information on this peptide using ESI−CID. Therefore, MALDI−PSD analysis was performed to discern between the two possible peptides (Figure 6B). The loss of H_3PO_4 (y_{20} − 98) was readily observed. However, only a few additional fragment ions were detectable. None of the observed fragments matched the peptide $Ser^{532}-Arg^{550}$. On the other hand, three of the fragment peaks matched the monophosphorylated peptide $Leu^{640}-Arg^{659}$. Since PAA analysis revealed that this HPLC fraction contained only phosphoserine amino acids, and since Ser^{654} is the only possible phosphorylation site on the peptide, we have provisionally assigned Ser^{654} as the phosphorylation site in MLK3.

Three of these MALDI peaks correspond to differential tryptic digestion products of the monophosphorylated peptide $Ser^{748}-Arg^{768}$ (at *m*/*z* 1940.73, $Ser^{748}-Arg^{766}$; at *m*/*z* 1272.55, $Ser^{758}-Arg^{768}$; and at *m*/*z* 1020.44, $Ser^{758}-Arg^{766}$). These sequences contain three Ser residues and two Thr residues. To determine the site of phosphorylation within this peptide, ESI−CID on fraction 27 was performed. Shown in Figure 6C is the CID spectrum of the doubly charged parent ion of *m*/*z* 1020.44. The most prominent peak corresponds to the neutral loss of H_3PO_4 (−49 Da) at *m*/*z* 461.2. Analysis of the COOH-terminal y ion fragmentation series rules out phosphorylation of Ser^{765}, since the masses of the y_5-y_8 ions do not contain the additional mass of a phosphate group.

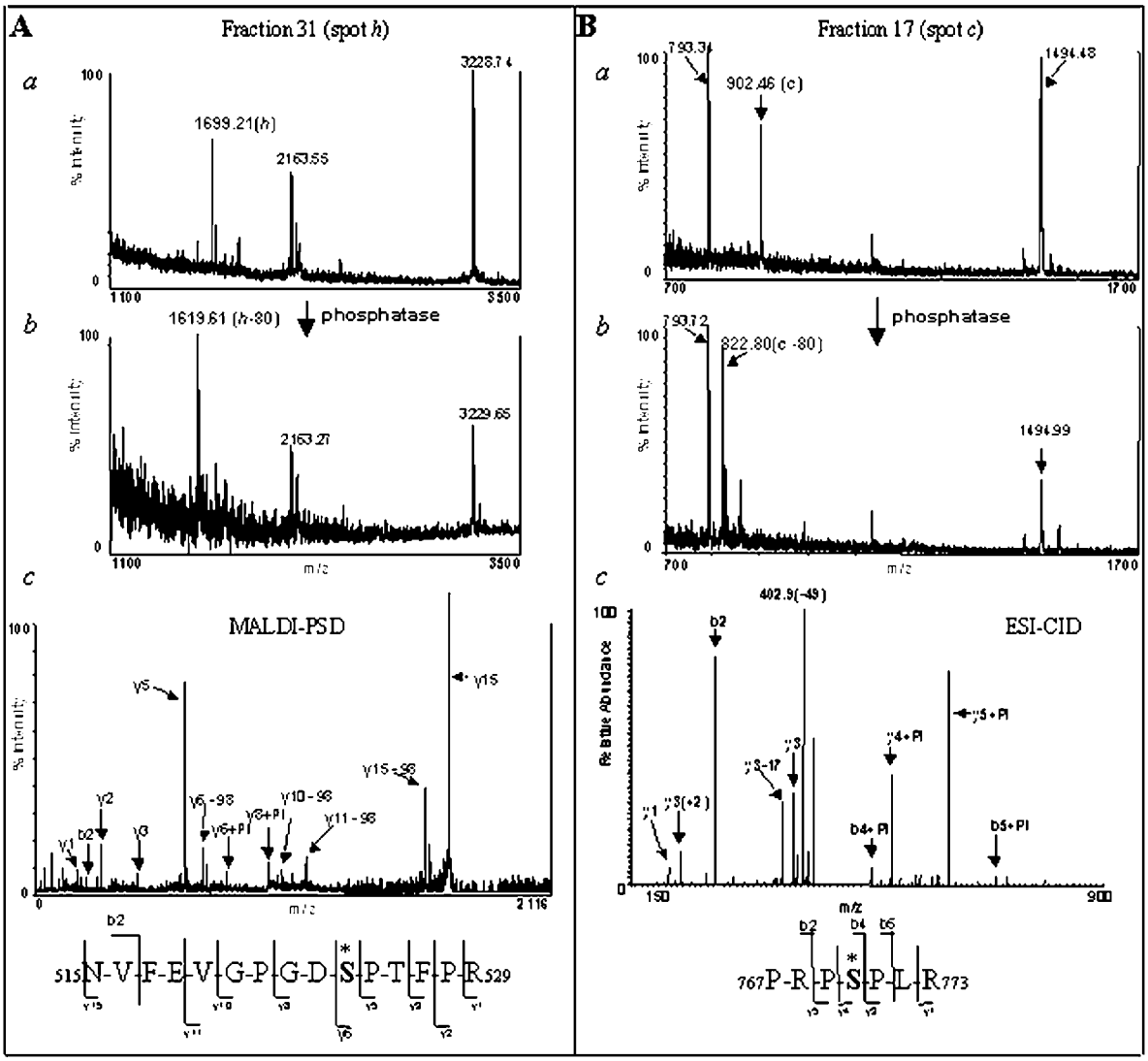

FIGURE 5: Analysis of HPLC fractions 31 and 17 by MALDI−PSD and ESI−CID. HPLC fractions 31(spot *h*) (A) and 17 (spot *c*) (B) were analyzed by MALDI-MS before (*a*) and after (*b*) phosphatase treatment. The *m*/*z* values corresponding to the phosphorylated and dephosphorylated MLK3 peptides are indicated in boldface. MALDI−PSD analysis was performed on fraction 31 (A, *c*). The fragment ions whose *m*/*z* value corresponds to y ions with the loss of H_3PO_4 (−98 Da) are labeled. ESI−CID of fraction 17 (B, *c*) was performed on an *m*/*z* value of 451.9, which corresponds to the doubly charged phosphorylated peptide Pro^{767}−Arg^{773}. The fragment ions whose *m*/*z* value corresponds to y or b ions with the addition of a phosphate group (Pi) are labeled. The observed fragment ions are indicated on the spectrum and peptide sequence (an asterisk indicates a phosphorylated residue).

Meanwhile, the mass of the b_2 ion indicates the presence of a phosphate group at Ser^{758}. Thus, Ser^{758} was assigned as a phosphorylation site in MLK3.

HPLC Fraction 20. The MALDI-MS spectra of fraction 20 (spot *d*) revealed a peak at 1329.16 that shifted by −80 Da to 1249.42 after phosphatase treatment. The phosphopeptide corresponded to a singly phosphorylated peptide Pro^{788}−Arg^{799} of MLK3 (Figure 7A, *a* and *b*). This sequence contains two Ser residues and no Thr residues. ESI−CID analysis of the doubly charged parent ion of *m*/*z* 662.5 revealed a predominant y series of fragment ions with a couple of b ions (Figure 7A, *c*). The neutral loss of H_3PO_4 was detected at *m*/*z* 613.4. The b_4 ion that contains Ser^{789} but not Ser^{793} corresponds to an *m*/*z* value expected for the unphosphorylated Ser residue. On the other hand, the *m*/*z* value of the y_7 ion corresponds to the sequence Ser^{793}−Arg^{799} containing a phosphate group, clearly identifying Ser^{793} as the phosphorylation site in a peptide contained in fraction 20.

HPLC Fraction 15. Fraction 15 contains spot *a*, the most intensely radiolabeled peptide on the two-dimensional phosphopeptide map (Figure 2A). MALDI-MS analysis of this fraction revealed a peak at *m*/*z* 1192.93, which shifted by −80 Da to *m*/*z* 1112.25 following phosphatase treatment (Figure 7B, *a* and *b*). This value corresponds to peptide Gly^{736}−Arg^{747} containing a single phosphate moiety. This peptide contains two Thr residues and two Ser residues. ESI−CID of the doubly charged parent ion revealed a predominant y series of fragment ions with a few b series ions (Figure 7B, *c*). The neutral loss of H_3PO_4 was detected at *m*/*z* 547.9. The y_7 fragment ion corresponds to an unphosphorylated MLK3 peptide fragment containing Thr^{745} and Ser^{746}. However, the y_8 fragment ion corresponds to a phosphorylated peptide fragment that contains Ser^{740}. These results identify Ser^{740} as the phosphorylation site on a peptide contained in fraction 15.

PGC Chromatography of Poorly Retained C18 Fractions. Fractions 1−7 eluted very early off the C-18 column in a

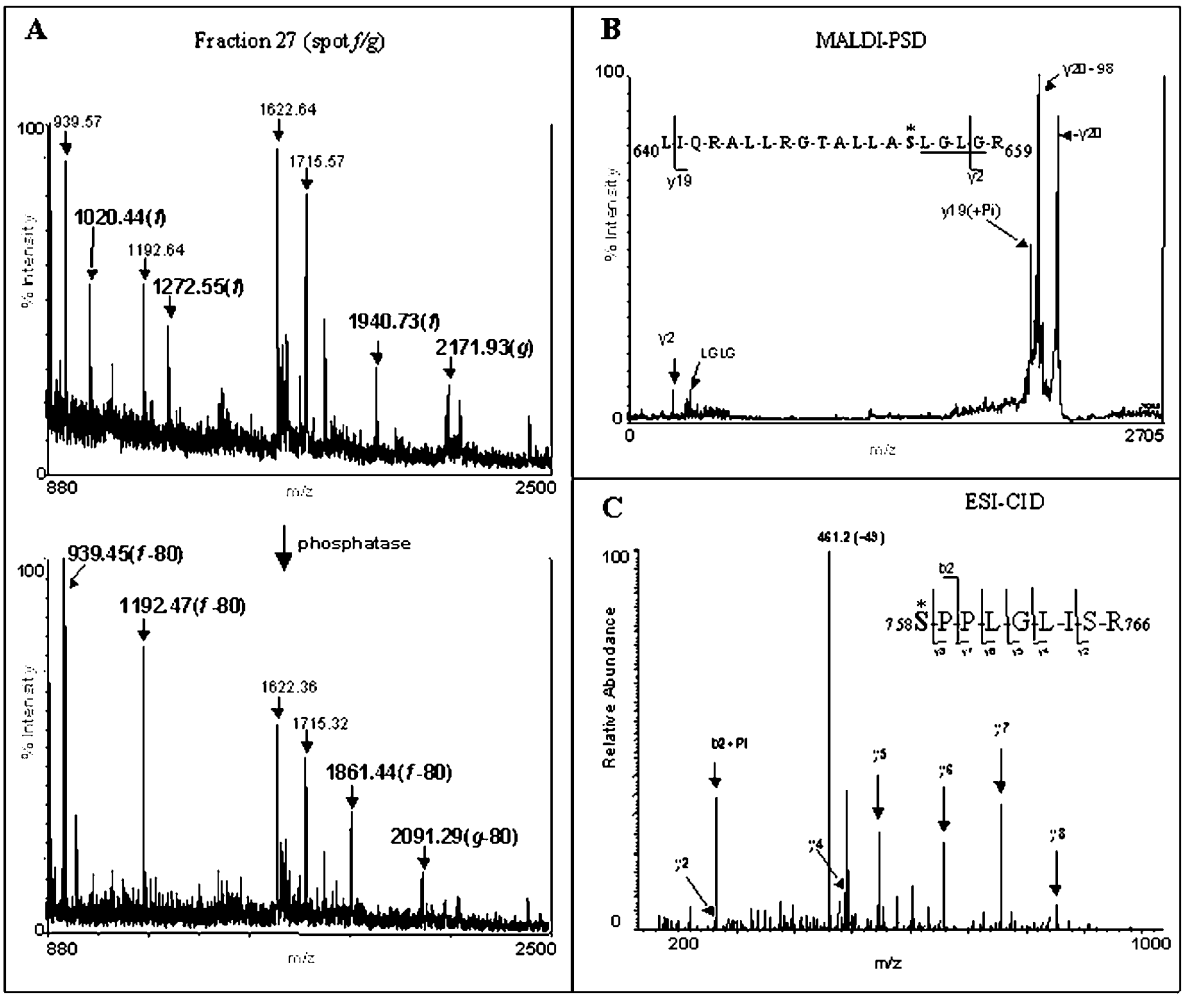

FIGURE 6: Analysis of HPLC fraction 27 using MALDI−PSD and ESI−CID. (A) HPLC fraction 27 (spots *f* and *g*) was analyzed by MALDI-MS before and following alkaline phosphatase treatment. The *m*/*z* values corresponding to phosphorylated and dephosphorylated peptides are indicated in boldface. (B) MALDI−PSD spectrum of the peptide at *m*/*z* 2172.93 in fraction 27. The y_{19} − 98 fragment ion corresponding to the loss of H_3PO_4 is indicated. (C) ESI−CID of the doubly charged parent ion at *m*/*z* 1020.44, which corresponds to the phosphorylated peptide Ser^{758}−Arg^{766} doubly charged. The fragment ions whose *m*/*z* value corresponds to y or b ions with the addition of a phosphate group (Pi) are labeled. The observed fragment ions are indicated on the spectrum and peptide sequence (an asterisk indicates a phosphorylated residue).

poorly resolved peak that contained contaminants such as salts and detergents. One-dimensional phosphopeptide mapping analysis showed that the Cdc42-inducible sites labeled *x* and *y* on the two-dimensional map eluted within this pool (Figure 2). Obtaining MALDI data for these HPLC fractions was not feasible, presumably due to signal repression caused by contaminants. To resolve these peptides from the contaminants, reverse-phase HPLC using a more hydrophobic resin, Porous Graphitic Carbon (PGC), was performed on the poorly retained C18 fractions. Figure 8A displays the chromatogram from the PGC analysis. The PGC column successfully retained and resolved multiple radiolabeled peptides that were present in the flowthrough fractions from the C18 column (Figure 8B). One-dimensional TLE and TLC analysis demonstrated that the radioactive fractions 22P−28P (where P indicates a fraction from the PGC column) contained the Cdc42-inducible sites (spots *x* and *y*) as well as spot *b* (Figure 8C).

MALDI-MS Analysis of PGC Fractions. PGC reverse-phase chromatography retained and resolved hydrophilic radiolabeled peptides, which were present in the poorly retained eluant from the C18 column. MALDI-MS analysis of these radiolabeled peptides is shown in Figure 9.

The MALDI-MS spectrum of fraction 23P contained a peak at *m*/*z* 805.39, which upon phosphatase treatment of the fraction followed by MALDI-MS showed a loss of −160 Da, corresponding to the loss of two phosphate groups (Figure 9A). Analysis of the calculated values indicated that the only possible tryptic phosphopeptide at this *m*/*z* value was Ser^{724}−Arg^{729}. This sequence contains two Ser residues and no Thr residues; thus, Ser^{724} and Ser^{727} were assigned as phosphorylation sites in MLK3.

Comparison of the mass spectra of fraction 28P before and after phosphatase treatment (Figure 9B) revealed a peak attributable to a monophosphorylated peptide. Based on the calculated values, Leu^{552}−Arg^{561} is the only possible tryptic phosphopeptide for the value at *m*/*z* 1242.36. This peptide contains two Ser residues and no Thr residues, and is an incompletely digested product. The completely digested tryptic peptide was identified in fraction 22P at *m*/*z* 1166.86 (Figure 9C), corresponding to Leu^{552}−Arg^{560} containing two phosphate moieties. Therefore, Ser^{555} and Ser^{556} were identi-

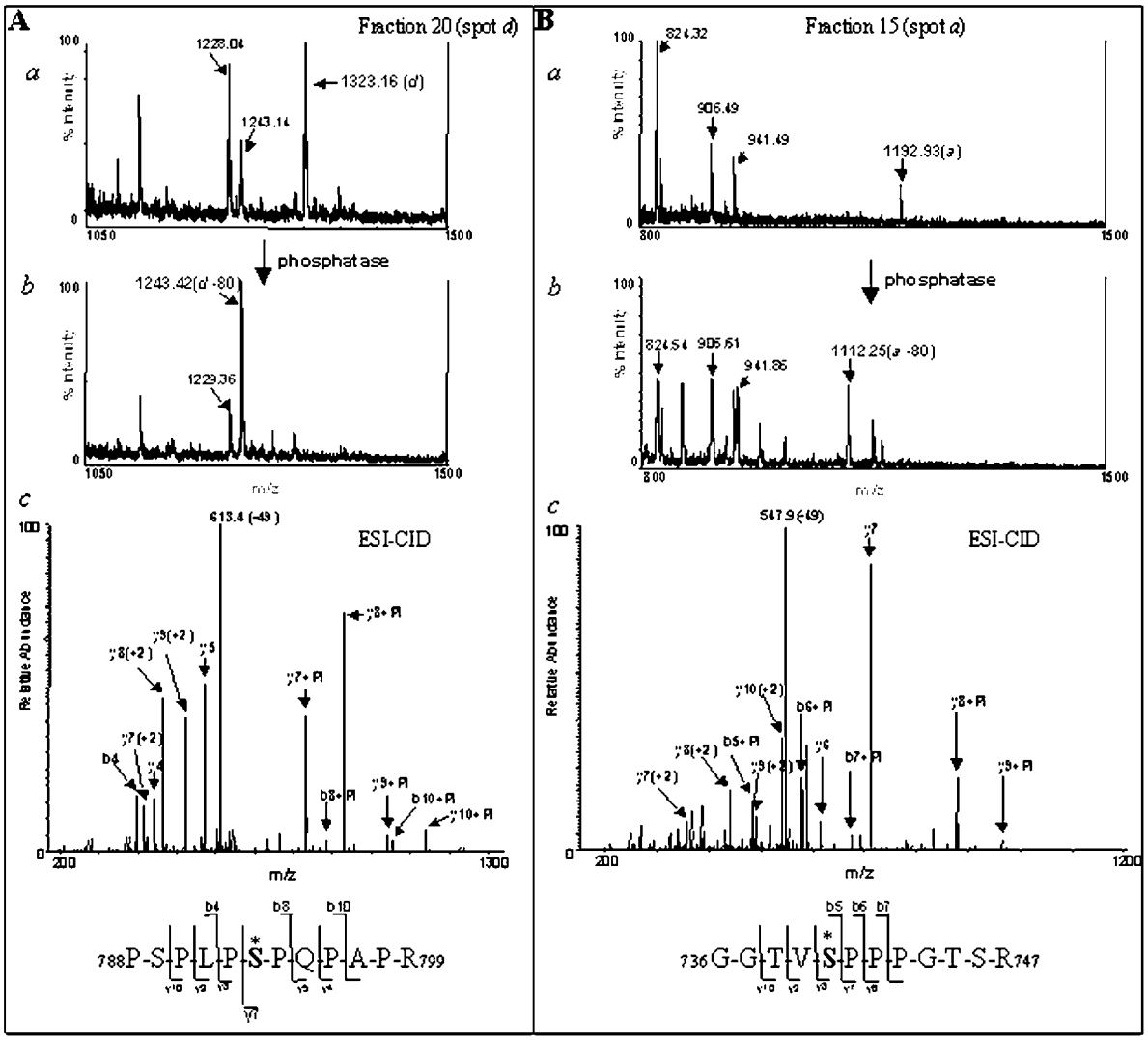

FIGURE 7: Analysis of HPLC fractions 20 and 15 by MALDI-MS and ESI−CID. HPLC fractions 20 (spot *d*) (A) and 15 (spot *a*) (B) were analyzed by MALDI-MS before (*a*) and after (*b*) phosphatase treatment. The *m*/*z* values corresponding to phosphorylated and dephosphorylated peptides are indicated in boldface. ESI−CID of fraction 20 (A, *c*) was performed on *m*/*z* 662.5. The fragment ions whose *m*/*z* value corresponds to y or b ions with the addition of a phosphate group (Pi) are labeled. ESI−CID of fraction 15 (B, *c*) was performed on *m*/*z* 597.1. The fragment ions whose *m*/*z* value corresponds to y or b ions with the addition of a phosphate group (Pi) are labeled. The observed fragment ions are indicated on the spectrum and peptide sequence (an asterisk indicates a phosphorylated residue).

fied as MLK3 phosphorylation sites that correspond to the Cdc42-inducible sites.

Comparative Two-Dimensional Phosphopeptide Mapping of in Vivo Labeled MLK3 Variants. To definitively correlate the identified phosphorylation sites from PGC chromatography with the spots on the two-dimensional map, phosphopeptide mapping was performed on in vivo labeled wild-type MLK3 or MLK3 phosphorylation site variants MLK3 S724A/S727A and MLK3 S555E/S556E. The MLK3 variants and Cdc42V12 were coexpressed in cells labeled with [^{32}P]orthophosphate. MLK3 was immunoprecipitated using an MLK3 polyclonal antibody, separated by SDS−PAGE, and transferred to a nitrocellulose membrane. Following trypsin digestion, the peptides were separated by two-dimensional TLE/TLC (Figure 10). Analysis of the two-dimensional map of MLK3 S724A/S727A clearly indicates that the diphosphorylated peptide containing phosphoSer^{724} and phosphoSer^{727} is represented by spot *b* on the map. Meanwhile, spots *x* and *y* are absent in the map of MLK3 S555E/S556E, indicating that spots *x* and *y* represent the products of differential trypsin digestion, and that Ser^{555} and Ser^{556} are Cdc42-induced phosphorylation sites on MLK3.

DISCUSSION

Many enzymes, including protein kinases, are regulated by reversible phosphorylation. Phosphorylation of a protein kinase can alter its catalytic activity, conformation, subcellular localization, and protein−protein interactions. To understand the function of a particular phosphorylation event, the precise site of in vivo phosphorylation must first be identified. The goal of this study was to map the in vivo sites of phosphorylation on MLK3 as a critical first step toward understanding the regulatory role of this posttranslational modification on MLK3 function. Using a combination of phosphopeptide mapping and mass spectrometry analysis, 12 in vivo phosphorylation sites have been identified.

Previous work in our lab has shown that MLK3 is multiphosphorylated in vivo, and that coexpression with activated Cdc42 (Cdc42V12) increases the in vitro catalytic

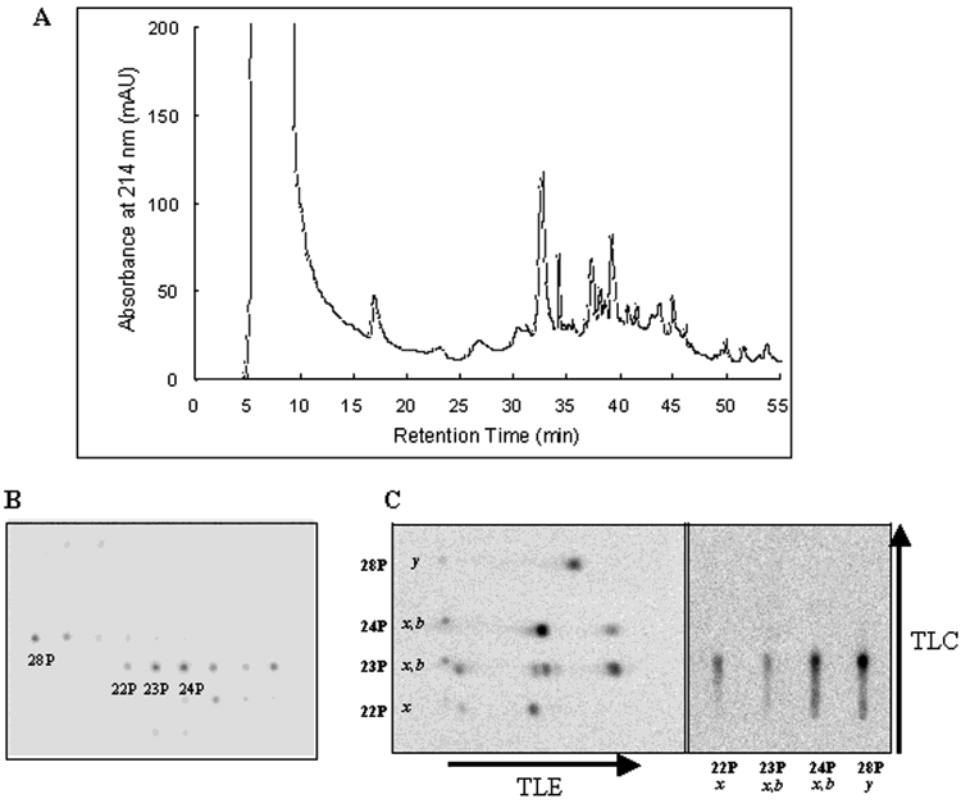

FIGURE 8: Fractionation of C18 flowthrough fractions by RP-HPLC on a Porous Graphitic Carbon column. (A) The C18 flowthrough fractions 1−7 were collected (Figure 2B), combined, and concentrated using a Speed Vac concentrator. The combined flowthrough sample was loaded onto the PGC column. Peptides were eluted by a linear acetonitrile gradient, and peak fractions were collected at approximately 1 min intervals. (B) Aliquots of each PGC fraction was spotted on a TLC plate and air-dried. Radiolabeled fractions were detected by phosphorimaging. (C) Aliquots of each radiolabeled PGC fraction was analyzed by one-dimensional TLE and one-dimensional TLC. For each radiolabeled PGC fraction, the elution number and the correlating spot(s) on the two-dimensional phosphopeptide map are indicated.

activity of MLK3 and alters its in vivo phosphorylation pattern (*23*). Therefore, cells coexpressing MLK3 and Cdc42 V12 were used as a model system to identify in vivo phosphorylation sites on MLK3, including those induced by Cdc42.

A portion of the cells was labeled with [^{32}P]orthophosphate to generate radiolabeled MLK3 for use as a tracer. This approach not only simplified selection of phosphopeptides, but also made it possible to assign phosphorylation sites to radiolabeled spots on the two-dimensional tryptic phosphopeptide map. Indeed, virtually all of the observed phosphopeptides in the map were identified using mass spectrometry. Thus, comparative two-dimensional phosphopeptide mapping should serve as a useful tool to study MLK3 phosphorylation in other model systems, such as the phosphorylation of endogenous MLK3 in response to different stimuli. A limitation of this approach is that the resulting radiolabeled phosphopeptides represent MLK3 phosphorylation events that occur only during the labeling period (the last 4 h of a 15 h transfection experiment). Since MLK3 expression is usually detected at around 8 h post-transfection, it is possible that very stable phosphorylation sites may have been missed using this approach.

However, an unforeseen advantage of using the radiolabeled tracer was the realization that the C18 column flowthrough fractions contained phosphorylated peptides, including those that represent Cdc42-inducible phosphorylation sites. Salts and other contaminants commonly found in the flowthrough fraction from C18 columns suppress the mass spectrometry signal (*28*). To overcome this problem, reverse-phase HPLC using a PGC column was used to desalt and partially resolve the C18 flowthrough fractions. PGC has been shown to be a more hydrophobic stationary phase than the C18 resin (*29*), and yet has the unique property of retaining very polar compounds. In addition, PGC chromatography has been used to resolve short and very hydrophilic peptides (*30*, *31*). The PGC HPLC successfully retained and resolved several peptides from the C18 flowthrough fractions, including the Cdc42-inducible phosphopeptides. Furthermore, the PGC column was used with the same volatile mobile phase as the C18 column, allowing for concentration of the sample and compatibility with mass spectrometry.

Following HPLC fractionation, the strategy to deduce phosphorylation sites was to first confirm which peptides from the radiolabel-containing HPLC fractions were phosphopeptides. MALDI-MS data were collected before and after alkaline phosphatase treatment. Using MALDI-MS, the loss of −80 Da after phosphatase treatment is diagnostic for loss of phosphate. In some cases, these data, in conjunction with PAA, were sufficient to assign the sites of phosphorylation. However, in several instances, the MALDI-MS data correlated to more than one MLK3 phosphopeptide or to MLK3 phosphopeptides that contained multiple Ser and Thr residues. These situations required MALDI−PSD analysis or ESI−CID mass spectrometry to attain sequence information and to unambiguously assign a site of phosphorylation. A surprising result from the ESI−CID analysis was the sequencing of three different phosphopeptides that resulted from trypsin cleaving Arg−Pro peptide bonds. Typically, trypsin is reported not to cleave Arg−Pro or Lys−Pro peptide

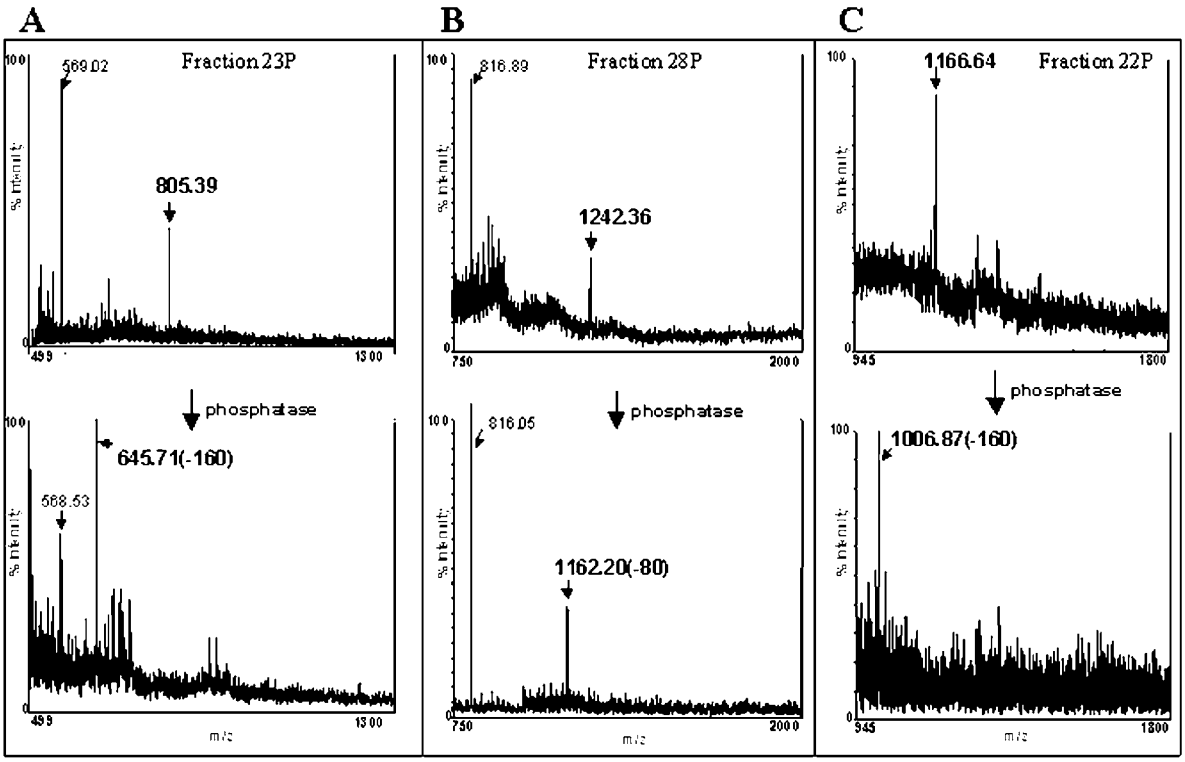

FIGURE 9: Analysis of PGC fractions using MALDI-MS combined with alkaline phosphatase treatment. PGC fractions 23P (A), 28P (B), and 22P (C) were analyzed by MALDI-MS in the linear positive ion mode. The *m*/*z* values corresponding to phosphorylated peptides are indicated in boldface. The PGC fractions were then subjected to alkaline phosphatase treatment and reanalyzed by MALDI-MS. The dephosphorylated peptides are indicated in boldface with the change in *m*/*z* of −80, or multiples thereof, corresponding to the loss of phosphate moieties.

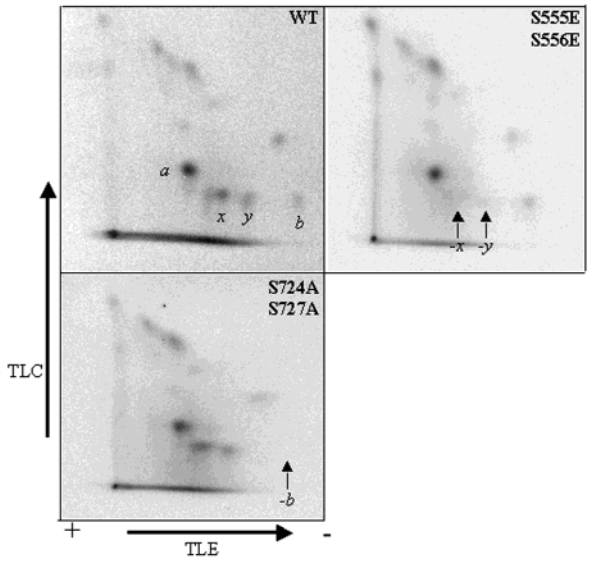

FIGURE 10: Two-dimensional maps of tryptic phosphopeptides derived from in vivo phosphorylated MLK3 variants. Cells expressing the specified MLK3 variants in the presence of Cdc42$^{Val\ 12}$ were incubated with [^{32}P]orthophosphate. MLK3 variants were immunoprecipitated from cellular lysates, blotted onto a nitrocellulose membrane (A), and subjected to trypsin digestion. (B) The resultant tryptic phosphopeptides were analyzed by comparative two-dimensional phosphopeptide analysis. Short arrows indicate tryptic phosphopeptides that are absent. Phosphopeptides were detected by phosphorimaging. Long arrows indicate the direction of electrophoresis and chromatography.

bonds (*32*−*34*), and most of the available computer programs used to generate tryptic peptides masses, including MS-Digest, do not take into account cleavage at Arg/Lys−Pro bonds. Possibly, something unique flanks these particular MLK3 sequences such as modification of the proline residue involved or isomerization of the peptide bond between Arg−Pro. Alternatively, uncommon cleavage may instead be due to the increased stability of the modified trypsin used in this study. Regardless, these results demonstrate that cleavage at Arg/Lys−Pro bonds should be considered in MS analysis of tryptic peptides.

The schematic location of the identified MLK3 in vivo phosphorylation sites is depicted in Figure 11. Other than a single phosphorylation site in the glycine-rich region (between amino acids 11 and 37), all of the identified phosphorylation sites cluster in two regions. Of the 12 sites, 7 are positioned between amino acids 650 and 800 in the COOH-terminal region of MLK3, while 3 phosphorylation sites, including the 2 Cdc42-inducible sites (Ser^{555} and Ser^{556}), are situated between amino acids 520 and 550 in the basic region immediately following the CRIB domain.

Knowledge of the sequence surrounding the phosphorylation site often provides valuable information as to the identity of the kinase responsible for the phosphorylation event. The majority of the sites identified in this study contain a Pro residue following the phosphorylation site, suggesting that MLK3 may be a target of proline-directed kinases. Proline-directed kinases, which include MAPKs, cyclin-dependent protein kinases (CDKs), and glycogen synthase kinase 3 (GSK3) among others, phosphorylate Ser/Thr residues that are immediately followed by a Pro residue (*35*). The peptide containing the Cdc42-inducible sites (Ser^{555}, Ser^{556}) does not contain a phosphoSer-Pro sequence, suggesting that phosphorylation of these sites is catalyzed by a

MALDI-MS

HPLC Fract.	2D spot	Peptide sequence	MH$^+$ Obs.	MH$^+$ Calc.	MH$^+$ after PTase Obs.	MH$^+$ after PTase Calc
15	*a*	$_{736}$GGTV**S**PPPGTSR$_{747}$	1192.93	1192.54	1112.25	1112.52
17	*c*	$_{767}$PRP**S**PLR$_{773}$	902.46	902.49	822.80	822.49
20	*d*	$_{788}$PSPLP**S**PQPAPR$_{799}$	1323.16	1323.66	1243.42	1243.66
23	*e*	$_{11}$SPLGSWNGSGS(G)$_{8}$RVEGSPK$_{37}$	2395.17	2395.08	2315.42	2315.08
27	*f/g*	$_{748}$SAPGTPGTPR **S**PPLGLISR$_{766}$	1940.73	1940.99	1861.44	1860.99
		$_{758}$**S**PPLGLISRPR$_{768}$	1272.55	1272.70	1192.47	1192.47
		$_{758}$**S**PPLGLISR$_{766}$	1020.44	1020.65	939.45	940.65
		$_{640}$LIQRALLRGTALLA **S**LGLGR$_{659}$	2171.93	2172.27	2091.29	2092.27
31	*h*	$_{515}$NVFEVGPGD**S**PTFPR$_{529}$	1699.21	1698.75	1619.61	1618.75
45	*i*	$_{702}$TPD**S**PPTPAPLLLDLGIPVGQR$_{723}$	2334.59	2334.21	2254.96	2254.21
22P	*x*	$_{552}$LED**SS**NGER$_{561}$	1166.64	1166.37	1006.87	1006.37
28P	*y*	$_{552}$LED**S**SNGERR$_{562}$	1242.36	1242.51	1162.20	1162.51
23P	*b*	$_{724}$**S**AK**S**PR$_{729}$	805.39	805.30	645.71	645.30

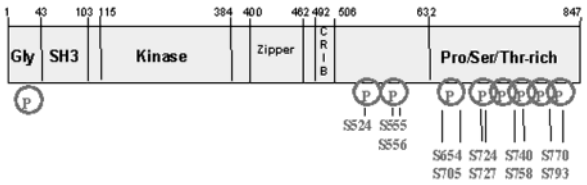

FIGURE 11: Schematic representation of MLK3 phosphorylation sites. (A) Table summarizing the observed (MALDI-MS) and calculated *m/z* values before and after alkaline phosphatase treatment for the identified phosphopeptides. (B) Block diagram of MLK3 indicating the location of the identified in vivo phosphorylation sites.

distinct family of kinases or is the result of MLK3 autophosphorylation.

The phosphorylation site Ser^{758}, located in the COOH-terminal tail of MLK3, resides in the sequence KSPRR and conforms to the stricter consensus sequence for the CDK family (KS/TP*X*R) (*36*). The phosphorylation site Ser^{705} exists in the sequence PDSP, and the phosphorylation site Ser^{757} exists in the sequence PRSP. These arrangements conform to the stricter consensus sequence for MAPK (including JNK) phosphorylation sites (P*X*S/TP) (*36*), leaving open the possibility that JNK might phosphorylate MLK3 in a potential feedback mechanism. Evidence for such a feedback mechanism has been demonstrated with the ERK pathway, where the MAPKKK Raf has been reported to be phosphorylated and activated by the MAPK ERK in response to insulin and other growth factors (*37*, *38*). Also, it has been shown that activated JNK can phosphorylate the COOH-terminal region of mixed-lineage kinase MLK2 (*39*), although no sites of phosphorylation were determined.

Due to the low abundance of phosphorylated signaling molecules in cells, determination of in vivo phosphorylation sites of protein kinases has been a difficult challenge. Recent improvements in the resolution and sensitivity of mass spectrometry instruments have made it more feasible to map protein phosphorylation sites from in vivo sources. In this study, a variety of mass spectrometry techniques were used to determine in vivo phosphorylation sites of the mixed-lineage kinase MLK3. Knowledge of the sequences that are modified provides the necessary first step into understanding how phosphorylation regulates MLK3 function.

REFERENCES

1. Ing, Y. L., Leung, I. W., Heng, H. H., Tsui, L. C., and Lassam, N. J. (1994) *Oncogene 9* (6), 1745−1750.
2. Gallo, K. A., Mark, M. R., Scadden, D. T., Wang, Z., Gu, Q., and Godowski, P. J. (1994) *J. Biol. Chem. 269* (21), 15092−15100.
3. Ezoe, K., Lee, S. T., Strunk, K. M., and Spritz, R. A. (1994) *Oncogene 9* (3), 935−938.
4. Tibbles, L. A., Ing, Y. L., Kiefer, F., Chan, J., Iscove, N., Woodgett, J. R., and Lassam, N. J. (1996) *EMBO J. 15* (24), 7026−7035.
5. Merritt, S. E., Mata, M., Nihalani, D., Zhu, C., Hu, X., and Holzman, L. B. (1999) *J. Biol. Chem. 274* (15), 10195−10202.
6. Liu, T. C., Huang, C. J., Chu, Y. C., Wei, C. C., Chou, C. C., Chou, M. Y., Chou, C. K., and Yang, J. J. (2000) *Biochem. Biophys. Res. Commun. 274* (3), 811−816.
7. Hirai, S., Katoh, M., Terada, M., Kyriakis, J. M., Zon, L. I., Rana, A., Avruch, J., and Ohno, S. (1997) *J. Biol. Chem. 272* (24), 15167−15173.
8. Davis, R. J. (2000) *Cell 103* (2), 239−252.
9. Yasuda, J., Whitmarsh, A. J., Cavanagh, J., Sharma, M., and Davis, R. J. (1999) *Mol. Cell. Biol. 19* (10), 7245−7254.
10. Kelkar, N., Gupta, S., Dickens, M., and Davis, R. J. (2000) *Mol. Cell. Biol. 20* (3), 1030−1043.
11. Hehner, S. P., Hofmann, T. G., Ushmorov, A., Dienz, O., Wing-Lan Leung, I., Lassam, N., Scheidereit, C., Droge, W., and Schmitz, M. L. (2000) *Mol. Cell. Biol. 20* (7), 2556−2568.
12. Hoffmeyer, A., Avots, A., Flory, E., Weber, C. K., Serfling, E., and Rapp, U. R. (1998) *J. Biol. Chem. 273* (17), 10112−10119.
13. Hoffmeyer, A., Grosse-Wilde, A., Flory, E., Neufeld, B., Kunz, M., Rapp, U. R., and Ludwig, S. (1999) *J. Biol. Chem. 274* (7), 4319−4327.
14. Hehner, S. P., Li-Weber, M., Giaisi, M., Droge, W., Krammer, P. H., and Schmitz, M. L. (2000) *J. Immunol. 164* (7), 3829−3836.
15. Maroney, A. C., Finn, J. P., Connors, T. J., Durkin, J. T., Angeles, T., Gessner, G., Xu, Z., Meyer, S. L., Savage, M. J., Greene, L. A., Scott, R. W., and Vaught, J. L. (2001) *J. Biol. Chem. 276* (27), 25302−25308.
16. Xu, Z., Maroney, A. C., Dobrzanski, P., Kukekov, N. V., and Greene, L. A. (2001) *Mol. Cell. Biol. 21* (14), 4713−4724.
17. Savinainen, A., Garcia, E. P., Dorow, D., Marshall, J., and Liu, Y. F. (2001) *J. Biol. Chem. 276* (14), 11382−11386.
18. Mota, M., Reeder, M., Chernoff, J., and Bazenet, C. E. (2001) *J. Neurosci. 21* (14), 4949−4957.
19. Bock, B. C., Vacratsis, P. O., Qamirani, E., and Gallo, K. A. (2000) *J. Biol. Chem. 275* (19), 14231−14241.
20. Vacratsis, P. O., and Gallo, K. A. (2000) *J. Biol. Chem. 275* (36), 27893−27900.
21. Zhang, H., and Gallo, K. A. (2001) *J. Biol. Chem. 276* (49), 45598−45603.
22. Burbelo, P. D., Drechsel, D., and Hall, A. (1995) *J. Biol. Chem. 270* (49), 29071−29074.
23. Bock, B. C., Vacratsis, P. O., Qamirani, E., and Gallo, K. A. (2000) *J. Biol. Chem. 275* (19), 14231−14241.
24. Teramoto, H., Coso, O. A., Miyata, H., Igishi, T., Miki, T., and Gutkind, J. S. (1996) *J. Biol. Chem. 271* (44), 27225−27228.
25. Leung, I. W., and Lassam, N. (2001) *J. Biol. Chem. 276* (3), 1961−1967.
26. Bock, B. C., Vacratsis, P. O., Qamirani, E., and Gallo, K. A. (2000) *J. Biol. Chem. 275* (May 12), 14231−14241.
27. Spengler, B., Kirsch, D., Kaufmann, R., and Jaeger, E. (1992) *Rapid Commun. Mass Spectrom. 6* (2), 105−108.
28. Roboz, J., Yu, Q., Meng, A., and van Soest, R. (1994) *Rapid Commun. Mass Spectrom. 8* (8), 621−626.
29. Ross, P., and Knox, J. H. (1997) *Adv. Chromatogr. 37*, 121−162.
30. Yamaki, S., Isobe, T., Okuyama, T., and Shinoda, T. (1996) *J. Chromatogr. A 729* (1−2), 143−153.
31. Chin, E. T., and Papac, D. I. (1999) *Anal. Biochem. 273* (2), 179−185.

32. Boyle, W. J., van der Geer, P., and Hunter, T. (1991) *Methods Enzymol. 201*, 110−149.
33. Hill, R. L. (1965) *Adv. Protein Chem. 20*, 37−107.
34. Carnegie, P. R. (1969) *Nature 223* (209), 958−959.
35. Hall, F. L., Braun, R. K., Mihara, K., Fung, Y. K., Berndt, N., Carbonaro−Hall, D. A., and Vulliet, P. R. (1991) *J. Biol. Chem. 266* (26), 17430−17440.
36. Songyang, Z., Lu, K. P., Kwon, Y. T., Tsai, L. H., Filhol, O., Cochet, C., Brickey, D. A., Soderling, T. R., Bartleson, C., Graves, D. J., DeMaggio, A. J., Hoekstra, M. F., Blenis, J., Hunter, T., and Cantley, L. C. (1996) *Mol. Cell. Biol. 16* (11), 6486−6493.
37. Lee, R. M., Cobb, M. H., and Blackshear, P. J. (1992) *J. Biol. Chem. 267* (2), 1088−1092.
38. Gardner, A. M., Vaillancourt, R. R., Lange-Carter, C. A., and Johnson, G. L. (1994) *Mol. Biol. Cell 5* (2), 193−201.
39. Phelan, D. R., Price, G., Liu, Y. F., and Dorow, D. S. (2001) *J. Biol. Chem. 276* (14), 10801−10810.

BI016075C